

Type of noise defines global attractors in bistable molecular regulatory systems

Joanna Jaruszewicz^a, Pawel J. Zuk^{a,b}, Tomasz Lipniacki^{a,c,*}

^a*Institute of Fundamental Technological Research, Polish Academy of Sciences, 02-106 Warsaw, Poland*

^b*Faculty of Physics, University of Warsaw, 00-681 Warsaw, Poland*

^c*Department of Statistics, Rice University, Houston, TX 77005, USA*

Abstract

The aim of this study is to demonstrate that in molecular dynamical systems with the underlying bi- or multistability, the type of noise determines the most strongly attracting steady state or stochastic attractor. As an example we consider a simple stochastic model of autoregulatory gene with a nonlinear positive feedback, which in the deterministic approximation has two stable steady state solutions. Three types of noise are considered: transcriptional and translational – due to the small number of gene product molecules and the gene switching noise – due to gene activation and inactivation transitions. We demonstrate that the type of noise in addition to the noise magnitude dictates the allocation of probability mass between the two stable steady states. In particular, we found that when the gene switching noise dominates over the transcriptional and translational noise (which is characteristic of eukaryotes), the gene preferentially activates, while in the opposite case, when the transcriptional noise dominates (which is characteristic of prokaryotes) the gene preferentially remains inactive. Moreover, even in the zero-noise limit, when the probability mass generically concentrates in the vicinity of one of two steady states, the choice of the most strongly attracting steady state is noise type-dependent. Although the epigenetic attractors are defined with the aid of the deterministic approximation of the stochastic regulatory process, their relative attractivity is controlled by the type of noise, in addition to noise magnitude. Since noise characteristics vary during the cell cycle and development, such mode of regulation can be potentially employed by cells to switch between alternative epigenetic attractors.

Keywords: gene expression, bistability, stochastic processes, epigenetic attractors

*Corresponding author

Email addresses: jjarusz@ippt.gov.pl (Joanna Jaruszewicz), pzuk@ippt.gov.pl (Pawel J. Zuk), tlipnia@ippt.gov.pl (Tomasz Lipniacki)

1. Introduction

From the mathematical perspective intracellular regulatory processes can be considered as stochastic dynamical systems. Stochasticity arises due to the limited number of reacting molecules such as gene copies, mRNA or proteins. In systems with underlying bistability, even for low noise, the stochastic trajectories exhibit stochastic jumps between basins of attraction and thus diverge qualitatively from the deterministic solutions. The relative stability of steady states depends on the system volume (or noise strength) [1]. In this study, we analyze the bistable stochastic system with three different types of noise and demonstrate that the dominating type of noise determines the most strongly attracting steady state (global stochastic attractor). That is, two systems with the same deterministic approximation may have qualitatively different stationary probability distributions (SPD) depending on the noise characteristic, even in the zero noise limit.

We consider two models of gene expression with autoregulation. We will assume that the gene is positively regulated by its own product in a cooperative manner, which leads to the nonlinear positive feedback and bistability. Single-cell experiments suggest that gene expression can be described by a three-stage model [2, 3]. The gene promoter can switch between two states [4, 5, 6], one active and one inactive. Such transitions could be associated with binding and unbinding of repressors or transcription factors or with changes in chromatin structure. Transcription can only occur if the promoter is active. The next two stages are mRNA transcription and protein translation. In certain cases when mRNA is very unstable and quickly translated, transcription and translation processes can be lumped together [7, 8]. The resulting model has thus two stages: gene regulation and protein synthesis. Such simplification allows for analytical treatment of the problem, however, lumping of transcription and translation processes may influence the impact of feedback on noise strength [9]. Therefore, in addition to the simplified two-stage model we analyze numerically a more detailed three-stage model in which processes of gene regulation, mRNA transcription and protein translation are explicitly included. The considered models have three types of noise: *transcriptional and translational* – due to the limited number of product molecules, and *gene switching* noise – due to gene state transitions.

Transcriptional and translational noises are characteristic for prokaryotes in which the mRNA and protein numbers are very small [10, 11, 12]. Recently, Taniguchi et al. quantified the mean expression of more than 1000 E. coli genes and found that the most frequent average protein number is of order of 10, while the most frequent average mRNA number is smaller than one [13]. The gene switching in prokaryotes is thought to be very fast and thus gene regulation is frequently considered in the so called adiabatic approximation [8], as a process that includes only mRNA transcription and protein translation [14, 15, 16].

Gene switching noise is important in eukaryotes [2, 4, 6, 17] in which the transitions between the *on* and *off* states are much less frequent. Analysis of gene expression in mammalian cells showed that mRNA is synthesized in bursts, during periods of time when the gene is transcriptionally active

[5]. Slow gene switching can result in bimodal mRNA and protein probability distributions even in systems without underlying bistability [8, 16]. Bimodality may arise also without bistability in two-stage cascades in which the regulatory gene produces transcription factors that have a nonlinear effect on the activity of the target gene [18]. In contrast to prokaryotes, in eukaryotes the characteristic mRNA and protein numbers are much larger. Therefore the transcriptional and translational noises in many cases may be neglected [19, 20, 21] or considered in the diffusion approximation [22, 7]. Cell cycle transcriptional regulator gene SWI6 in yeast is an example of a gene with expression noise originating almost only from gene switching noise, while transcriptional noise is negligible [23].

The bistable regulatory elements received a lot of attention in the last decade as they enhance heterogeneity and may allow cells in multicellular organism to specialize and specify their fate. Decisions between cell death, survival, proliferation and senescence are associated with bistability and stochasticity, magnitude of which controls transition rates between the particular attractors [24, 25, 26]. In prokaryotes the bistability is regarded as an optimal strategy for coping with infrequent changes in the environment [27].

The simplest regulatory element exhibiting bistability is the self-regulating gene controlled by a nonlinear positive feedback [8, 28, 29, 30, 31, 32]. While not often found as an isolated entity, the self-regulating gene is a common element of biological networks; for example, 40% of *E. coli* transcription factors negatively regulate their own transcription [33]. Sinderen et al. demonstrated that transcription factor *comK* acts as an autoregulatory switch in *Bacillus subtilis* [34]. The synthetic auto-regulatory eukaryotic gene switch was studied in *Saccharomyces cerevisiae* [35]. The other intensively studied regulatory element exhibiting bistability is the toggle switch – a pair of mutual repressors [36, 37]. A classical example is the double-negative regulatory circuit governing alternative lysogenic and lytic states of phage lambda [38], lactose utilization network [39] or Delta-Notch regulation [40].

Despite the low copy number of proteins and mRNAs genetic switches may exhibit very low transition rates, resulting in stable epigenetic properties that persist in simplest organisms for many generations [38, 41], reviewed by [37]. The attractors of genetic networks can be associated with distinct cell types achieved during cell differentiation [41, 42]. In single cell, in the long time scale the relative occupancy of steady states is determined by their relative stability. The same, however, may not be true for cell population when the two steady states are associated with different growth rates. As demonstrated, by Nevozhay et al. using synthetic bistable gene circuit, the fraction of cells in the most strongly attracting steady state may be low, if these cells have lower growth rate than cells in the less stable steady state [43]. Thus, in the context of cell population the relative occupancy of a given state is defined by rates of state to state transitions (or memory) and fitness associated with particular steady states.

The paper is organized as follows: in the following section we consider the two-stage gene autoregulation model and its three approximations:

- the deterministic approximation

- the continuous approximation with the gene switching noise only,
- and the adiabatic approximation with the transcriptional and translational noise only.

Based on two last approximations, we demonstrate that the type of noise determines the global attractor. Then, we numerically calculate the SPD in the case when two types of noise are present and show that the most strongly attracting steady state is determined by the prevalent type of noise. For a relatively large subdomain in the parameter space, the SPD is concentrated either in one or the other stable steady state depending on the dominating type of noise. We supplement our consideration of the two-stage model by analysis of SPD following from Langevin equations in which the white noise term is added to the equation obtained in the deterministic approximation.

Finally, to confirm our findings, we consider a more detailed, three-stage model in which processes of gene regulation, mRNA transcription and protein translation are explicitly included, which enables distinguishing of transcriptional and translational noises. Within the latter model we demonstrate that the global attractor is determined by relative magnitudes of the transcriptional and gene switching noises, while the translational noise is the least important. We conclude discussing these two types of noise in the context of gene expression in bacteria and eukaryotes.

2. RESULTS

2.1. Two-stage model and its approximations

We assume that the gene may be in one of the two states – active or inactive, Fig. 1A. In this model we assume that the protein is synthesized directly from the gene, with the rate constant Q only when the gene is active and is degraded with the rate constant r . We chose time units in which $r = 1$. The rate constant Q is proportional to the product of transcription and translation rate constants Q_1 and Q_2 . The autoregulation arises when gene activation and/or inactivation rates ($c(Y)$ and $b(Y)$) depend on the level of synthesized protein Y . The model defines a time continuous Markov process described by two random variables: the gene state $G(t) \in \{0, 1\}$ and number of protein molecules $Y(t) \in \mathbb{N}$. The resulting transition propensities are

$$\begin{cases} G = 0 \rightarrow G = 1 & c(Y), \\ G = 1 \rightarrow G = 0 & b(Y), \\ Y = n \rightarrow Y = n + 1 & QG, \\ Y = n \rightarrow Y = n - 1 & n. \end{cases} \quad (1)$$

Let g_n denote the probability that $\{G, Y\} = \{1, n\}$ and h_n denote the probability that $\{G, Y\} = \{0, n\}$. Probabilities g_n and h_n follow a countable set of chemical master equations

$$\begin{cases} \frac{dg_n}{dt} = Q(g_{n-1} - g_n) + (n + 1)g_{n+1} - ng_n + c(n)h_n - b(n)g_n, \\ \frac{dh_n}{dt} = (n + 1)h_{n+1} - nh_n - c(n)h_n + b(n)g_n, \end{cases} \quad (2)$$

where we set $g_{-1} = 0$ to close the first of Eqs. (2).

Here, we focus on such $c(n)$ and $b(n)$ that define the positive nonlinear autoregulation leading to bistability. Thus, we assume

$$c(n) = c_0 + (c_2/Q^2)n^2, \quad b(n) = b_0 \quad \text{with} \quad c_0, c_2, b_0 > 0. \quad (3)$$

Such type of regulation arises in the case when the gene is switched on by its own product in a cooperative manner or by the other transcription factor present at some constant level. In order to analyze systems with various average numbers of proteins, but having the same deterministic limit, the nonlinear term $(c_2/Q^2)n^2$ is scaled by Q , which is equivalent to the assumption that the gene switching rates are proportional to the protein concentration rather than to the protein number.

Even in the stationary case, the system (2) can be solved analytically using a moment generating function only in the case when $c(n)$ and $b(n)$ are both constant, or one of them is constant and the other is linear in n [8]. In our case (3), due to the second order nonlinearity in $c(n)$, the method proposed in [8] leads to the third order ordinary differential equation, we failed to solve. We will thus estimate the marginal SPD $f_n = g_n + h_n$ corresponding to the exact model by Monte Carlo simulations of the system (1). Analytically, we will study three approximations to the exact model: the continuous approximation with the gene switching noise only, the adiabatic approximation with the transcriptional noise only, and the deterministic approximation, Fig. 1B.

2.1.1. Deterministic approximation

This classical approximation [44] is justified when the transition rates $c(n)$ and $b(n)$ are much greater than one, and simultaneously the characteristic number of protein molecules is very large. In such a case one may consider $y = Y/Q$ as a continuous variable. The scaled protein level $y(t)$ is given by a single ordinary differential equation

$$\frac{dy}{dt} = G(y) - y, \quad \text{where} \quad G(y) = \frac{c(y)}{c(y) + b(y)}. \quad (4)$$

In our specific case, $c(y) = c_0 + c_2y^2$ and $b(y) = b_0$, thus the stationary solutions of the equation (4) are the real roots of the third order polynomial

$$W = -c_2y^3 + c_2y^2 - (c_0 + b_0)y + c_0 = 0. \quad (5)$$

We will focus on the bistable case when W has three real roots such that $0 < y_1 < y_2 < y_3 < 1$. Steady states y_1 and y_3 are stable, while y_2 is unstable. Due to the fact that W has the same coefficient at the third and the second power, its roots satisfy $y_1 + y_2 + y_3 = 1$. The original coefficients b_0, c_0, c_2 may be recovered from the roots by the following relations:

$$c_0 = \frac{b_0 y_1 y_2 y_3}{y_1(y_2 + y_3) + y_2 y_3(1 - y_1)}, \quad c_2 = \frac{b_0}{y_1(y_2 + y_3) + y_2 y_3(1 - y_1)}. \quad (6)$$

Due to relation $y_3 = 1 - y_1 - y_2$, the (y_1, y_2, y_3) parameter space may be reduced to the domain $D \ni \{y_1, y_2\}$ such that $y_1 < y_2$ and $1 - y_1 - y_2 = y_3 > y_2$.

2.1.2. Continuous approximation

The model with noise resulting only from gene switching was analyzed previously in [29]. When the characteristic number of protein molecules is very large, as in the deterministic case, $y = Y/Q$ may be considered a continuous variable which follows

$$\frac{dy}{dt} = G - y, \quad (7)$$

where G , as in the exact model, is given by the process (1). These assumptions define a time continuous piece-wise deterministic Markov process. Probabilities $g_n(t)$ and $h_n(t)$ are now replaced by the continuous functions $g(y, t)$, $h(y, t)$, that satisfy [19, 21]

$$\frac{\partial h}{\partial t} - \frac{\partial}{\partial y}(yh) = b(y)g - c(y)h, \quad (8)$$

$$\frac{\partial g}{\partial t} + \frac{\partial}{\partial y}((1-y)g) = -b(y)g + c(y)h. \quad (9)$$

The above system has the following stationary solution [30]

$$h(y) = \exp \left[\int \left(\frac{-b(y)}{(1-y)} + \frac{c(y)-1}{y} \right) dy \right], \quad g(y) = \frac{yh(y)}{(1-y)}. \quad (10)$$

In our specific case, when $c(y) = c_0 + c_2 y^2$ and $b(y) = b_0$, the marginal SPD $f(y) = g(y) + h(y)$ may be expressed analytically:

$$f(y; c_2, c_0, b_0) = C e^{\frac{1}{2}c_2 y^2} y^{c_0-1} (1-y)^{b_0-1}, \quad (11)$$

where C is such that $\int_0^1 f(y) = 1$.

Now, we will replace original coefficients b_0, c_0, c_2 by y_1, y_2 (see Eq. 6) and introduce $\sigma := 1/b_0$. Let us note that for such defined σ all gene switching noise rates b_0, c_0, c_2 are inversely proportional to σ . The coefficient σ is an inverse of the adiabaticity coefficient, introduced in [8], and will be referred to as a measure of gene switching noise. Specifically, we will consider the SPD in the limit $\sigma \rightarrow 0$. In this limit the SPD given by Eq. 11 converges either to the Dirac delta in y_1 or in y_3 , i.e. to $\delta(y_1)$, or to $\delta(y_3)$ for all $\{y_1, y_2\} \in D$, except $\{y_1, y_2\}$ such that

$$\lim_{\sigma \rightarrow 0} \frac{f(y_1; y_1, y_2, \sigma)}{f(y_3; y_1, y_2, \sigma)} := C_1, \quad \text{where } 0 < C_1 < \infty. \quad (12)$$

Eqs. 6, 11 and 12 define (in the implicit form) the separatrix $S_{\text{continuous}}$

$$\left(\frac{1-y_1}{y_1+y_2}\right)\left(\frac{y_1}{1-y_1-y_2}\right)^{p_1} e^{p_2} = 1, \quad (13)$$

where

$$p_1 = \frac{y_1 y_2 (1 - y_1 - y_2)}{(1 - y_1)(1 - y_2)(y_1 + y_2)}, \quad p_2 = \frac{2y_1 + y_2 - 1}{2(1 - y_1)(y_1 + y_2)}. \quad (14)$$

That is, in the continuous approximation, the bistability domain D is split by the separatrix $S_{\text{continuous}}$ (on which $0 < C_1 < \infty$) into two subdomains. For $\{y_1, y_2\}$ above the separatrix $S_{\text{continuous}}$ $C_1 = \infty$ and the SPD converges to $\delta(y_1)$ as $\sigma \rightarrow 0$, while for $\{y_1, y_2\}$ below the separatrix $S_{\text{continuous}}$ $C_1 = 0$ and the SPD converges to $\delta(y_3)$, see Fig. 2A.

Simulations of the stochastic process in the continuous approximation, i.e. simulation of a piecewise continuous process given by Eqs. 1 and 7, were performed using the Haseltine and Rowlings algorithm [45, 20]. These simulations show significantly different behavior of the protein level $y(t)$ near each of the two stable stationary points (see Figs. 3C and 3D). When the trajectory is in the vicinity of y_1 (Fig. 3D) the characteristic time for which the gene is switched off $\sim 1/c(y_1)$ is much longer than the characteristic time for which the gene is switched on $\sim 1/b_0$. When the trajectory is in the vicinity of y_3 (Fig. 3C) these two times are similar. The characteristic departures from both states y_1 and y_3 are larger towards y_2 than in the opposite direction. For low noise there are relatively few transitions through the unstable state y_2 . The frequency of these transitions decreases to zero with decreasing noise.

2.1.3. Adiabatic approximation

This approximation is justified when transition rates $c(n)$ and $b(n)$ are much larger than the protein degradation rate constant. In such a case, G may be replaced [8, 46] by its expected value $G = G(n) = c(n)/(c(n) + b(n))$. This approximation leads to a birth-death process with birth and death propensities:

$$\begin{aligned} B(n) &= G(n)Q, \\ D(n) &= n. \end{aligned} \quad (15)$$

As in the case of the continuous approximation, the simulations show that trajectories near each stable stationary point differ significantly, Fig. 4. The birth and death events are less frequent near y_1 than near y_3 .

Let F_n denote the stationary probability that the number of protein molecules is equal to n . In the steady state the net probability current between neighboring states N and $N + 1$ is equal to zero, i.e.

$$F_n B(n) - F_{n+1} D(n + 1) = 0, \quad (16)$$

which gives F_n in the form

$$F_n = F_0 \prod_{i=0}^{n-1} \frac{B(i)}{D(i+1)}. \quad (17)$$

Eq. 17 defines the discrete probability density function F_n when $\sum_{n=1}^{\infty} \left(\prod_{i=0}^{n-1} \frac{B(i)}{D(i+1)} \right) < \infty$, which is satisfied provided that for sufficiently large j , $\frac{B(i)}{D(i+1)} < a < 1$ for all $i > j$. Since $\frac{B(i)}{D(i+1)} < Q/n$, the last condition holds. Now, we may choose F_0 such that $\sum_{n=0}^{\infty} F_n = 1$. We analyze the discrete probability density F_n for small $\varepsilon = 1/Q$. In the limit of $\varepsilon \rightarrow 0$, the adiabatic approximation converges to the deterministic approximation, and so the coefficient ε will be considered as a measure of transcriptional and translational noise. Let $F^Q(y) := QF_n$, where $y := n/Q$, i.e. $F^Q(y) = QF^Q(0) \prod_{i=1}^{yQ-1} \frac{\mathbf{b}(i/Q)}{\mathbf{d}(i/Q+1/Q)}$, where $\mathbf{b}(i/Q) := B(i)$, $\mathbf{d}(i/Q) := D(i)$. Now,

$$\log F^Q(y) = \log Q + \log F^Q(0) + \sum_{i=1}^{yQ-1} \log \frac{\mathbf{b}(i/Q)}{\mathbf{d}(i/Q + 1/Q)}. \quad (18)$$

In the limit of $\varepsilon \rightarrow 0$, $\mathbf{d}(i/Q + 1/Q) \rightarrow \mathbf{d}(i/Q)$. Next, replacing the sum by the integral, we obtain

$$\log F^Q(y) = \log Q + \log F^Q(0) + Q \int_0^y \log \frac{\mathbf{b}(z)}{\mathbf{d}(z)} dz, \quad (19)$$

thus

$$F^Q(y) = QF^Q(0) \exp \left(Q \int_0^y \log \frac{\mathbf{b}(z)}{\mathbf{d}(z)} dz \right). \quad (20)$$

Since $\int_0^{\infty} F^Q(z) dz = 1$ we get

$$F^Q(y) = \frac{\exp(Q\phi(y))}{\int_0^{\infty} \exp(Q\phi(z)) dz}, \quad (21)$$

where

$$\phi(y) = \int_0^y \log \frac{\mathbf{b}(z)}{\mathbf{d}(z)} dz. \quad (22)$$

The Laplace's method implies that in the limit of $Q \rightarrow \infty$, the function $F^Q(y)$ converges to the Dirac delta distribution $\delta(y_m)$ in the unique global maximum y_m of $\phi(y)$, provided that such global maximum exists. In our case $\mathbf{b}(y) = Q(c_0 + c_2 y^2)/(c_0 + c_2 y^2 + b_0)$ and $\mathbf{d}(y) = Qy$. Using Eqs. 6 and 22 we obtain

$$\begin{aligned}
\phi(y) &= 2\sqrt{y_1 y_2 y_3} \arctan\left[\frac{y}{\sqrt{y_1 y_2 y_3}}\right] - \\
&\quad - 2\sqrt{y_2 y_3 + y_1(y_3 + y_2)} \arctan\left[\frac{y}{\sqrt{y_2 y_3 + y_1(y_3 + y_2)}}\right] + \\
&\quad + y\left(1 + \log\left[\frac{y_1 y_2 y_3 + y^2}{y(y_2 y_3 + y_1(y_3 + y_2) + y^2)}\right]\right).
\end{aligned} \tag{23}$$

Since the extrema of $F^Q(y)$ coincide with the extrema of $\phi(y)$, the global maximum of $\phi(y)$ is either in y_1 or y_3 , thus the SPD converges either to $\delta(y_1)$ or to $\delta(y_3)$ as $Q \rightarrow \infty$. Only in the non-generic case, in which $\phi(y)$ has no global maximum, i.e. when

$$\phi(y_1) = \phi(y_3) \tag{24}$$

the SPD converges to the sum of two Dirac delta functions $A_1\delta(y_1) + A_3\delta(y_3)$. Eqs. 23 and 24 define the separatrix $S_{\text{adiabatic}}$. For $\{y_1, y_2\}$ above the separatrix $S_{\text{adiabatic}}$ the SPD converges to $\delta(y_1)$, while for $\{y_1, y_2\}$ below the separatrix $S_{\text{adiabatic}}$ the SPD converges to $\delta(y_3)$ as $\varepsilon \rightarrow 0$, Fig. 2A. The allocation of probability mass depends also on the magnitude of noise. In Fig. 2B we show the separatrices, (defined as lines $y_2(y_1)$ on which the SPD is equally distributed between the two basins of attraction) obtained from Eq. 17 for two values of ε . The separatrices converge to $S_{\text{adiabatic}}$ as $\varepsilon \rightarrow 0$.

2.2. SPD dependence on the transcriptional and gene switching noise magnitudes

Simulations in the continuous and adiabatic models (see Figs. 3 and 4) were both performed for point $C = \{y_1 = 0.03, y_2 = 0.27\}$ in parameter space shown in Fig. 2A. For the continuous approximation the characteristic departures from the stable steady states y_1 and y_3 are of similar magnitude. The case of the adiabatic approximation is different. Here, the fluctuations around point y_3 are much larger than around point y_1 . This suggests that the average time spent in the vicinity of point y_1 before the transition to point y_3 will be longer than the average time spent in the vicinity of point y_3 before the reverse transition. As a result the SPD for the adiabatic approximation will concentrate around point y_1 , while for the continuous approximation the SPD will concentrate around y_3 . This effect should be even more pronounced in the low noise limit when the transitions between the two attractors are less frequent. Accordingly, as shown in Fig. 2A the separatrices $S_{\text{adiabatic}}$ and $S_{\text{continuous}}$ are different, and together they bound domain \mathcal{C} , such that in the zero noise limit for $\{y_1, y_2\} \in \mathcal{C}$, the SPD of the continuous model converges to $\delta(y_1)$, while the SPD of the adiabatic model converges to $\delta(y_3)$. In the further analysis we consider the three sets of roots shown in Fig. 2A, i.e.

$$\begin{aligned}
A &= \{0.1, 0.35\} \in \mathcal{A}, \\
B &= \{0.15, 0.25\} \in \mathcal{B},
\end{aligned}$$

$$C = \{0.03, 0.27\} \in \mathcal{C}.$$

In Fig. 5, we compare the SPD of the adiabatic and of the continuous approximations. For $\{y_1, y_2\} = A$ and $\{y_1, y_2\} = B$ the SPDs obtained in both approximations are concentrated (in the low noise limit) in the vicinity of the same steady state, y_1 and y_3 , respectively for A and B . However, for $\{y_1, y_2\} = C$, the SPD of the adiabatic approximation is concentrated in the vicinity of y_1 , while the SPD of the continuous approximation is concentrated in the vicinity of y_3 . Let us also note that in case B the magnitude of noise controls the relative allocation of probability mass between basins of attraction of steady states y_1 and y_3 .

In the adiabatic approximation the gene switching noise σ is, by definition, identically 0. Similarly, in the continuous approximation the transcriptional and translational noise ε is identically 0. We thus showed that in the parameter subdomain \mathcal{C} the system settles in the inactive state for $\varepsilon/\sigma = \infty$ (adiabatic approximation) and settles in the active state for $\varepsilon/\sigma = 0$ (continuous approximation). This suggests that there exist a range of parameters for which noise ratio ε/σ determines which of the two steady states is the most strongly attracting. We now verify this conjecture considering the exact model with different ε and σ values, see Fig. 6. To estimate the SPD we performed long-run Monte Carlo simulations of the system (1) using the Gillespie algorithm [47]. For the analysis shown in Fig. 6, we chose $C = \{0.03, 0.27\} \in \mathcal{C}$. Such a choice of $\{y_1, y_2\}$ produces the equimodal SPD in the case when magnitudes of transcriptional and gene switching noises are comparable (and sufficiently large), i.e. $\varepsilon = 1/300$ and $\sigma = 1/100$. We observe that when magnitude of the transcriptional or gene-switching noise decreases to zero the SPD becomes unimodal. As expected from the analysis shown in Fig. 5, the SPD is concentrated in y_1 as $\sigma \rightarrow 0$ (adiabatic approximation limit), and in y_3 as $\varepsilon \rightarrow 0$ (continuous approximation limit). Therefore, we demonstrated when two types of noise are present, their relative magnitudes determine the global attractor. This effect has an analog in equilibrium selection in evolutionary games [48].

2.3. Langevin approach

The classical approach to complex stochastic systems involves Langevin equation in which various noise sources are replaced by white, which magnitude is either constant (additive noise) or is a function of the solution (multiplicative noise), in the simplest case is proportional to the solution (as in geometric Brownian motion equation). Here, we follow this procedure starting from the deterministic approximation of our model. Langevin-Ito equation extending deterministic equation 4 is

$$\frac{dy}{dt} = A(y) + \xi(t)\sqrt{B(y)/V}, \quad \text{where } A(y) := G(y) - y, \quad (25)$$

and $\xi(t)$ is a Gaussian white noise, with

$$\langle \xi(t) \rangle = 0, \quad \langle \xi(t)\xi(t') \rangle = \delta(t - t'). \quad (26)$$

In this description $\sqrt{B(y)/V}$ is identified as noise intensity, where V is the volume of the reactor. In the case of additive noise $B(y) = \text{const} = B_0$. We consider also the case of multiplicative noise, assuming that its magnitude is proportional to $y(t)$ and set $B(y) = y$. The other choice of multiplicative noise was made by Frigola et al. [49], who assumed that magnitude of noise is proportional to the sum of birth and death rates (in our case it would be $G(y) + y$). One should notice that such a choice is in a sense arbitrary since adding any function $f(y)$ to birth and death rates, leaves deterministic equation unchanged but changes its stochastic counterpart.

The Fokker-Planck equation corresponding to the above Langevin-Ito equation reads [22]

$$\frac{\partial F(y, t)}{\partial t} = -\frac{\partial}{\partial y}((A(y))F(y, t)) + \frac{1}{2V} \frac{\partial^2}{\partial y^2}(B(y)F(y, t)). \quad (27)$$

In the stationary case ($\partial F(y, t)/\partial t = 0$) this equation solves explicitly to

$$F(y) = \frac{CV}{B(y)} \text{Exp}(-2V\phi(y)), \quad (28)$$

where $\phi(y)$

$$\phi(y) = -\int_0^y \frac{A(z)}{B(z)} dz \quad (29)$$

has the meaning of potential. In the case of additive noise, $B(y) = B_0$, $\phi(y)$ is proportional to deterministic potential $\phi(y) = -\int_0^y (A(z))dz$. Analogously to previous section the separatrices S_{additive} and $S_{\text{multiplicative}}$ are given in implicit form by $\phi(y_1) = \phi(y_3)$. In Fig. 7 we show them together with previously determined separatrices $S_{\text{adiabatic}}$ and $S_{\text{continuous}}$ in y_1, y_2 plane. In order to calculate these two new separatrices, we make use of Eqs. 6 giving c_0 and c_2 as functions of y_1, y_2 and y_3 .

The alternative way of calculating separatrices S_{additive} and $S_{\text{multiplicative}}$ involves the, so called, Dynkin equation (dual to Fokker-Plank equation) for the first mean passage time (MFPT) $T_{\theta, \gamma}(y)$ from y to the absorbing boundary at $y = \theta$, with the reflective boundary at $y = \gamma$ (see book of Gardiner [50] for the MFPT introduction, and [43, 49] for the recent relevant application of this method):

$$-1 = A(y) \frac{\partial T_{\theta, \gamma}(y)}{\partial y} + \frac{1}{2V} B(y) \frac{\partial^2 T_{\theta, \gamma}(y)}{\partial y^2}. \quad (30)$$

The boundary conditions are $T_{\theta, \gamma}(\theta) = 0$, and $dT_{\theta, \gamma}/dy = 0$ at $y = \gamma$. In the low noise limit, the probability mass fraction concentrated in the vicinity of steady state y_1 is $(T_{3 \rightarrow 1})/(T_{3 \rightarrow 1} + T_{1 \rightarrow 3})$, where $T_{1 \rightarrow 3}$ is the MFPT from y_1 to y_3 and $T_{3 \rightarrow 1}$ is the MFPT from y_3 to y_1 . To calculate $T_{1 \rightarrow 3}$ we set $\theta = y_3$ and $\gamma = 0$, while to calculate $T_{3 \rightarrow 1}$ we set $\theta = y_1$ and $\gamma = \infty$. Our separatrices are given by equality $T_{3 \rightarrow 1} = T_{1 \rightarrow 3}$ in $V \rightarrow \infty$ limit. Obviously, MFPTs give more information than just the probability mass allocation as they account for cell memory, [43]. Times $T_{1 \rightarrow 3}$ and $T_{3 \rightarrow 1}$ may be obtained in explicit integral forms from the equation 30 [50].

In summary, using the classical Langevin approach we confirmed that prediction of the most strongly attracting steady state, strongly depends on assumed noise, here, either additive or multiplicative. As one could expect, the additive noise separatrix closely matches with that of continuous approximation in which noise results solely from gene switching, while the multiplicative noise separatrix closely match with that of the adiabatic approximation for which the magnitude of noise grows with the number of molecules. As already said, in original stochastic model the most strongly attracting steady state is determined by relative magnitude of gene switching, transcriptional and translational noises, and thus in general it may not be predicted basing on Langevin equation in which all noise sources are lumped together and replaced by white noise. By considering arbitrary noise functions we showed recently, that any steady state can become a global stochastic attractor for particular choice of noise [51].

2.4. Three-stage model

In this section we consider a more detailed model of an autoregulatory gene and demonstrate that the choice of the most strongly attracting steady state is governed by the relative magnitudes of gene switching, transcriptional and translational noises. The following three processes are included in the model: the gene activation/inactivation, mRNA transcription and protein translation, Fig. 8. The mRNA is synthesized with the rate constant Q_1 and is degraded with the rate constant r_1 . The protein is translated on the mRNA template with the rate constant Q_2 and is degraded with the rate constant r_2 . The transcriptional and translational noise are characterized, respectively, by parameters $\varepsilon_1 = r_1/Q_1$ and $\varepsilon_2 = r_2/Q_2$. Thus the characteristic number of proteins (achieved when the gene is turn on for infinitely long time) is equal to $N = 1/(\varepsilon_1\varepsilon_2)$. As in the previous model we assume that the gene may be in one of two states: inactive $G = 0$ (no mRNA synthesis), or $G = 1$ – active due to binding of its own protein or some transcription factor implicitly present in the model at constant concentration. The transition from state $G = 0$ to $G = 1$ proceeds with rate $c_0 + (c_2/N^2)Y^2$, (where Y is the number of proteins), while the transition from $G = 1$ to $G = 0$ proceeds with constant rate b_0 . The coefficient c_2 describing cooperative autoactivation scales with N^2 , which is equivalent to the assumption that protein binding rate is proportional to the concentration rather than to the number of molecules. It is assumed that the cell size is proportional to the characteristic protein number N . As in the previous model the gene switching noise is characterized by the parameter $\sigma = 1/b_0$. The model defines a time continuous Markov process described by three random variables: the gene state $G(t) \in \{0, 1\}$, number of mRNA molecules $X(t) \in \mathbb{N}$ and number of proteins $Y(t) \in \mathbb{N}$.

The assumed reaction rate constants are listed in the Table 1. For a non-dimensional analysis we chose time units in which $r_2 = 1$ (third column). Parameter values for prokaryotes and eukaryotes are calculated by assuming $r_2 = 10^{-4}/\text{s}$. As discussed in the Introduction, prokaryotes are characterized by large transcriptional and translational noise, while eukaryotes have larger gene switching noise. Therefore, in the example shown in Fig. 9, we assume for bacteria $\varepsilon_1 = \varepsilon_{01}$, $\varepsilon_2 = \varepsilon_{02}$, $\sigma = \sigma_0/100$ and for eukaryotes $\varepsilon_1 = \varepsilon_{01}/5$, $\varepsilon_2 = \varepsilon_{02}/25$, $\sigma = \sigma_0$, where $\varepsilon_{01} = 1/15$, $\varepsilon_{02} = 1/75$ and $\sigma_0 =$

1/50. Parameters ε_{01} , ε_{02} and σ_0 , will be referred to as default parameters. They are so chosen that the SPD corresponding to the Markov process is bimodal, and the probability mass is equally distributed between two basins of attraction, Fig. 9A. Fig. 10 shows stochastic simulation trajectory corresponding to the SPD shown in Fig. 9A.

In the $\sigma \rightarrow 0$, $\varepsilon_1 \rightarrow 0$ and $\varepsilon_2 \rightarrow 0$ limit, the considered Markov process for $X(t)$, $Y(t)$ can be approximated by the system of two ordinary differential equations for scaled variables $x(t) = \varepsilon_1 X(t)$, $y(t) = \varepsilon_1 \varepsilon_2 Y(t)$

$$\frac{dx}{dt} = r_1(\overline{G}(y) - x) \quad \text{where} \quad \overline{G}(y) = \frac{c_0 + c_2 y^2}{c_0 + c_2 y^2 + b_0}, \quad (31)$$

$$\frac{dy}{dt} = r_2(x - y). \quad (32)$$

In a relatively broad range of parameters the above system exhibits bistability. The stable steady states with high and low protein concentration will be referred to as active and inactive, respectively. For assumed parameters (Table 1) the three steady states are:

Inactive: $x_1 = 0.03$, $y_1 = 0.03$;

Unstable: $x_2 = 0.26$, $y_2 = 0.26$;

Active: $x_3 = 0.71$, $y_3 = 0.71$.

Let us note that stationary solutions of the system (31-32) depend only on c_0/b_0 and c_2/b_0 , i.e. are independent to noise parameters σ , ε_1 , ε_2 . Noise parameters, however, influence the SPD. As shown in Fig. 9, the SPD for default noise parameters (Table 1) is bimodal with the probability mass equally distributed between two basins of attraction, Fig. 9A. Decrease of the gene switching noise σ (with the transcriptional and translational noises kept constant) causes that probability mass concentrates in the inactive state, Fig. 9B. In contrast, decrease of the transcriptional noise ε_1 (with the gene switching and translational noises kept constant) causes that the probability mass concentrates in the active state, Fig. 9C. Decrease of the translational noise (simultaneously with transcriptional noise) does not significantly influence the SPD, Fig. 9D. Considering this observation, we focus on the normalized transcriptional to gene switching noise ratio, defined as $R = \frac{\varepsilon_1/\varepsilon_{01}}{\sigma/\sigma_0}$. In Fig. 11 we analyze the mass fraction of the SPD in the basin of attraction of the inactive state, S_1 , as a function of R . Fraction S_1 approaches unity as $R^{-1} \rightarrow 0$ (for fixed ε_1 and ε_2) and approaches zero as $R \rightarrow 0$ (for fixed σ). The results presented in Figs. 9 and 11 demonstrate that the type of dominating noise determines the most strongly attracting steady state. The small R (transcriptional to gene switching noise ratio), characteristic for eukaryotes, promotes gene activation. In turn, large R , characteristic for bacteria, promotes gene inactivation.

3. CONCLUSIONS

We considered two models of a self-regulating gene with underlying bistability. In the simplified two-stage model, the transcription and translation processes were lumped together, which allowed for the analytical approach. Next, we considered the three-stage model with three types of noise; transcriptional and translational – due to the limited number of mRNA and protein molecules, and the gene-switching noise – due to gene activation and inactivation. Analysis of both models demonstrated that the relative magnitudes of transcriptional and translational, and gene switching noise determine how the SPD is allocated between the two basins of attraction. We found that the low ratio of transcription to gene switching noise (R) promotes gene activation, while large R promotes gene inactivation.

Behavior of living cells is inherently associated with noise, which can be either perceived as an obstacle to accurate signal processing, or as a necessary factor introducing heterogeneity in cell populations. Noise enables cells to explore the state space, and allocates the cell population between the local optima - the epigenetic attractors. In this study we demonstrated that in the given epigenetic landscape, defined by the deterministic approximation, the relative occupancy of the attractors is controlled by the type of noise, even in the limit in which noise amplitude converges to zero. The theoretical consequence of our finding is that the prediction of the most strongly attracting steady state or global attractor in the classical Langevin approach, in which all noise sources are replaced by white noise, may not, in general, be correct. Observation that the most strongly attracting steady state, is controlled by relative contributions of the gene switching and transcriptional noise may be exploited in synthetic biology, which enables controlling the magnitudes of different noise sources in designed systems; see eg. [11, 12] where transcription and translation rates were independently modulated.

As already said the dominant noise is cell type-specific. The process of gene expression, analyzed in this study, involves at least three types of noise: gene-switching, transcriptional and translational. Eukaryotic and prokaryotic cells differ significantly in their gene expression noise characteristics. In eukaryotes, the most important source of noise are infrequent transitions between the *on* and *off* states [5, 23]. In turn due to a large volume and correspondingly a large number of mRNA and proteins, the transcriptional and translational noises are relatively low. In the model the larger number of mRNA and protein was achieved by the increase of mRNA transcription and protein translational rate constants, which reflects the higher number of mRNA polymerases and ribosomes in eukaryotic cells. In prokaryotic cells gene activation and deactivation are thought to be very fast due to small volume, which implies easier contact and more frequent binding of transcription factors to the gene promoters. Thus, the gene switching noise in prokaryotes is typically low. Due to the small number of mRNA molecules and proteins, the gene expression noise in prokaryotic cells originates mostly from the transcription and translation events [13]. As a result eukaryotes, compared with prokaryotes, have a lower ratio of transcriptional to gene switching noise, which as

demonstrated in this study promotes activation of autoregulatory genes.

In our study we concentrate on the the gene expression noise, which is the most ubiquitous, but not always dominant source of noise in cell signaling. Earlier, we theoretically then experimentally demonstrated that at low dose $\text{TNF}\alpha$ stimulation, noise associated with stochastic receptor activation dominates over gene expression noise in $\text{NF-}\kappa\text{B}$ system [20, 52]. As a result, at low dose stimulation, individual cell responses became highly asynchronous, with fraction of responding cells decreasing with the stimulation dose [52, 53].

Noise characteristics are not only cell type-specific, but may also change during the cell cycle and development. This opens the possibility that relative occupancy of steady states may be actively controlled by noise. For example cell volume growth in G_1 phase and DNA replication in S phase asynchronously modify the relative contributions of gene switching, transcriptional and translational noises. Much larger changes in noise magnitude and its characteristics accompany embryogenesis in fruit fly or frog. In the first case nuclear divisions (mitoses) begin following fertilization, but are not accompanied by division of cytoplasm (cytokinesis). Only after thirteen mitotic divisions, the approximately 6000 nuclei are partitioned into separate cells [54]. In the case of frog embryogenesis the huge egg is converted into a tadpole consisting of millions of much smaller cells containing the same amount of organic matter [55]. One might speculate that changes in noise magnitude and characteristics add to the formation of morphogen gradients (changing relative stability of predefined steady states) initiating body segmentation and cell differentiation. Such mode of control, would require a more precise tuning of parameters than the simple tilting of the epigenetic landscape. However, it would have the advantage of keeping the epigenetic attractors (potentially the most plausible states) unchanged, with simultaneous modification of their relative occupancy.

ACKNOWLEDGMENTS

We thank Dr Marek Kimmel for helpful comments. This study was supported by the Foundation for Polish Science grant TEAM/2009-3/6, Polish Ministry of Science and Higher Education grant N N501 132936 and NSF/NIH grant No. R01-GM086885.

REFERENCES

- [1] M. Vellela, H. Qian, Stochastic dynamics and non-equilibrium thermodynamics of a bistable chemical system: the Schloegl model revisited, *J. R. Soc. Interface* 6 (2009) 925–40. (page 2)
- [2] W.J. Blake, M. Kaern, C.R. Cantor, J.J. Collins, Noise in eukaryotic gene expression, *Nature* 422 (2003) 633–637. (pages 2, 21)
- [3] J.M. Raser, E.K. O’Shea, Control of stochasticity in eukaryotic gene expression, *Science* 304 (2004) 1811–1814. (page 2)
- [4] M.S.H. Ko, Stochastic model for gene induction, *J. Theor. Biol.* 153 (1991) 181–194. (page 2)

- [5] A. Raj, C.S. Peskin, D. Tranchina, D.Y. Vargas, S. Tyagi, Stochastic mRNA synthesis in mammalian cells, *PLoS Biol.* 4 (2006) 1707-1719. (pages 2, 3, 14, 21)
- [6] J.R. Chubb, T. Treck, S.M. Shenoy, R.H. Singer, Transcriptional pulsing of a developmental gene, *Curr. Biol.* 16 (2006) 1018-1025. (page 2)
- [7] T.B. Kepler, T.C. Elston, Stochasticity in transcriptional regulation: origins, consequences, and mathematical representations, *Biophys. J.* 81 (2001) 3116-3136. (pages 2, 3)
- [8] J.E.M. Hornos, D. Schultz, G.C.P. Innocentini, J. Wang, A.M. Walczak, J.N. Onuchic, P.G. Wolynes, Self-regulating gene: An exact solution, *Phys. Rev. E.* 72 (2005) 051907. (pages 2, 3, 5, 6, 7)
- [9] T.T. Marquez-Lago, J. Stelling, Counter-intuitive stochastic behavior of simple gene circuits with negative feedback, *Biophys. J.* 98 (2010) 1742-1750. (page 2)
- [10] H.H. McAdams, A. Arkin, Stochastic mechanisms in gene expression, *Proc. Natl. Acad. Sci. USA*, 94 (1997) 814-819. (page 2)
- [11] A.M. Kierzek, J. Zaim, P. Zielenkiewicz, The effect of transcription and translation initiation frequencies on the stochastic fluctuations in prokaryotic gene expression, *J. Biol. Chem.* 276 (2001) 8165-8172. (pages 2, 14)
- [12] E.M. Ozbudak, M. Thattai, I. Kurtser, A.D. Grossman, A. Oudenaarden, Regulation of noise in the expression of a single gene, *Nat. Genet.* 31 (2002) 69-73. (pages 2, 14)
- [13] Y. Taniguchi, P.J. Choi, G.W. Li, H. Chen, M. Babu, J. Hearn, A. Emili, X.S. Xie, Quantifying E. coli proteome and transcriptome with single-molecule sensitivity in single cells, *Science* 329 (2010) 533-538. (pages 2, 14, 21)
- [14] M. Thattai, A. Oudenaarden, Intrinsic noise in gene regulatory networks, *Proc. Natl. Acad. Sci. USA*. 98 (2001) 8614-8619. (page 2)
- [15] P.S. Swain, M.B. Elowitz, E.D. Siggia, Intrinsic and extrinsic contributions to stochasticity in gene expression, *Proc. Natl. Acad. Sci. USA*. 99 (2002) 12795-12800. (page 2)
- [16] V. Shahrezaei, P.S. Swain, Analytical distributions for stochastic gene expression, *Proc. Natl. Acad. Sci. USA*. 105 (2008) 17256-17261. (pages 2, 3)
- [17] A. Raj, A. Oudenaarden, Single-molecule approaches to stochastic gene expression, *Annu. Rev. Biophys.* 38 (2009) 255-270. (page 2)
- [18] A. Ochab-Marcinek, M. Tabaka, Bimodal gene expression in noncooperative regulatory systems, *Proc. Natl. Acad. Sci. USA*. 107 (2010) 22096-22101. (page 3)
- [19] T. Lipniacki, P. Paszek, A. Marciniak-Czochra, A.R. Brasier, M. Kimmel, Transcriptional stochasticity in gene expression, *J. Theor. Biol.* 238 (2006) 348-367. (pages 3, 6)
- [20] T. Lipniacki, K. Puszynski, P. Paszek, A.R. Brasier, M. Kimmel, Single TNF α trimers mediating NF- κ B activation: stochastic robustness of NF- κ B signaling, *BMC Bioinformatics* 8 (2007) 376. (pages 3, 7, 15)
- [21] A. Bobrowski, T. Lipniacki, K. Pichór, R. Rudnicki, Asymptotic behavior of distributions of mRNA and protein levels in a model of stochastic gene expression, *J. Math. Anal. Appl.* 333 (2007) 753-769. (pages 3, 6)

- [22] N.G. van Kampen, *Stochastic processes in physics and chemistry*, 3rd ed. Elsevier Science & Technology Books, 2007. (pages 3, 11)
- [23] A. Becksei, B.B. Kaufmann, A. van Oudenaarden, Contributions of low molecule number and chromosomal positioning to stochastic gene expression, *Nat. Genet.* 37 (2005) 937–944. (pages 3, 14)
- [24] J. Hasty, J. Pradines, M. Dolnik, J.J. Collins, Noise-based switches and amplifiers for gene expression, *Proc. Natl. Acad. Sci. USA.* 97 (2000) 2075–2080. (page 3)
- [25] K. Puszynski, B. Hat, T. Lipniacki, Oscillations and bistability in the stochastic model of p53 regulation, *J. Theor. Biol.* 254 (2008) 452–465. (page 3)
- [26] T. Lipniacki, B. Hat, J.R. Faeder, W.S. Hlavacek, Stochastic effects and bistability in T cell receptor signaling, *J. Theor. Biol.* 254 (2008) 110–122. (page 3)
- [27] E. Kussell, S. Leibler, Phenotypic diversity, population growth, and information in fluctuating environments, *Science* 309 (2005) 2075–2078. (page 3)
- [28] A.M. Walczak, J.N. Onuchic, P.G. Wolynes, Absolute rate theories of epigenetic stability, *Proc. Natl. Acad. Sci. USA* 102 (2005) 18926–18931. (page 3)
- [29] R. Karmakar, I. Bose, Positive feedback, stochasticity and genetic competence, *Phys. Biol.* 4 (2007) 29–37. (pages 3, 6)
- [30] B. Hat, P. Paszek, M. Kimmel, K. Piechor, T. Lipniacki, How the number of alleles influences gene expression, *J. Stat. Phys.* 128 (2007) 511–533. (pages 3, 6)
- [31] D. Schultz, J.N. Onuchic, P.G. Wolynes, Understanding stochastic simulations of the smallest genetic networks, *J. Chem. Phys.* 126 (2007) 245102. (page 3)
- [32] D. Siegal-Gaskins, E. Grotewold, G.D. Smith, The capacity for multistability in small gene regulatory networks, *BMC Syst. Biol.* 3 (2009) 96. (page 3)
- [33] N. Rosenfeld, M. Elowitz, U. Alon, Negative autoregulation speeds the response times of transcription networks, *J. Mol. Biol.* 323 (2002) 785–793. (page 3)
- [34] D. van Sinderen, G. Vemnema, comK acts as an autoregulatory control switch in the signal transduction route to competence in *Bacillus subtilis*, *J. Bacteriology* 176 (1994) 5762–5770. (page 3)
- [35] A. Becskei, B. Seraphin, L. Serrano, Positive feedback in eucaryotic gene networks: cell differentiation by graded to binary response conversion, *EMBO J.* 20 (2001) 2528–2535. (page 3)
- [36] A. Lipshtat, A. Loinger, N.Q. Balaban, O. Biham, Genetic toggle switch without cooperative binding, *Phys. Rev. Lett.* 96 (2006) 188101. (page 3)
- [37] A. Chatterjee, Y.N. Kaznessis, W.-S. Hu, Tweaking biological switches through a better understanding of bistability behavior, *Curr. Opin. Biotechnol.* 19 (2008) 475–481. (page 3)
- [38] M. Ptashne, *A genetic switch: phage lambda revisited*, 3rd ed., Cold Harbor Spring Laboratory Press, 2004. (page 3)
- [39] E.M. Ozbudak, M. Thattai, H.N. Lim, B.I. Shraiman, A. Oudenaarden, Multistability in the lactose utilization network of *Escherichia coli*, *Nature* 427 (2004) 737–740. (page 3)

- [40] D. Sprinzak, A. Lakhanpal, L. Lebon, L.A. Santat, M.E. Fontes, G.A. Anderson, J. Garcia-Ojalvo, M.B. Elowitz, Cis-interactions between Notch and Delta generate mutually exclusive signalling states, *Nature* 465 (2010) 86–90. (page 3)
- [41] M. Acar, A. Becskei, A. van Oudenaarden, Enhancement of cellular memory by reducing stochastic transitions, *Nature* 435 (2005) 228–232. (page 3)
- [42] H.H. Chang, P.Y. Oh, D.E. Ingber, S. Huang, Multistable and multistep dynamics in neutrophil differentiation, *BMC Cell. Biol.* 7 (2006) 11. (page 3)
- [43] D. Nevozhay, R.M. Adams, E. Van Itallie, M.R. Bennett, G. Balazsi, Mapping the Environmental Fitness Landscape of a Synthetic Gene Circuit, *PLoS Comput. Biol.* 8 (2012) e1002480. (pages 3, 11)
- [44] G.K. Ackers, A.D. Johnson, M.A. Shea, Quantitative model for gene regulation by λ phage repressor, *Proc. Natl. Acad. Sci. USA* 79 (1982) 1129–1133. (page 5)
- [45] E.L. Haseltine, J.B. Rawlings, Approximate simulation of coupled fast and slow reactions for stochastic chemical kinetics, *J. Chem. Phys.* 117 (2002) 6959–6969. (page 7)
- [46] A. Bobrowski, Degenerate convergence of semigroups related to a model of stochastic gene expression, *Semigroup Forum* 73 (2006) 345–366. (page 7)
- [47] D.T. Gillespie, Exact stochastic simulation of coupled chemical reactions, *J. Phys. Chem.* 81 (1977) 2340–2361. (page 10)
- [48] J. Miekisz, Equilibrium selection in evolutionary games with random matching of players, *J. Theor. Biol.* 232 (2005) 47–53. (page 10)
- [49] D. Frigola, L. Casanellas, J. M. Sancho, M. Ibanes, Asymmetric Stochastic Switching Driven by Intrinsic Molecular Noise, *PLoS One* 7 (2012) e31407. (page 11)
- [50] C.W. Gardiner, *Handbook of stochastic methods for physics, chemistry and the natural sciences*. Berlin: Springer-Verlag, 2004. (page 11)
- [51] P.J. Zuk, M. Kočańczyk, J. Jaruszewicz, W. Bednorz, T. Lipniacki, Dynamics of a stochastic spatially extended system predicted by comparing deterministic and stochastic attractors of the corresponding birth–death process, *Phys. Biol.* 9 (2012) 055002. (page 12)
- [52] S. Tay, J. Hughey, T. Lee, T. Lipniacki, S.R. Quake, M.W. Covert, Single-cell NF- κ B dynamics reveal digital activation and analogue information processing. *Nature* 466 (2010) 267–271. (page 15)
- [53] D.A. Turner, P. Paszek, D.J. Woodcock, D.E. Nelson, C.A. Horton, Y. Wang, D. G. Spiller, D. A. Rand, M.R.H. White, C.V. Harper Physiological levels of TNF α stimulation induce stochastic dynamics of NF- κ B responses in single living cells. *J Cell Sci* 123 (2010) 2834–2843. (page 15)
- [54] J.A. Campos-Ortega, *The embryonic development of Drosophila melanogaster*, second ed., Springer, 1997. (page 15)
- [55] P.D. Nieuwkoop, J. Faber, *Normal Table of Xenopus laevis (Daudin)*, Garland Publishing Inc, New York & London, 1994. (page 15)
- [56] K.P. Jayapal, S. Sui, R.J. Philp, Y.-J. Kok, M.G.S. Yap, T.J. Griffin, W.-S. Hu, Multitagging Proteomic Strategy to Estimate Protein Turnover Rates in Dynamic Systems, *J. Proteome Res.* 9 (2010) 2087–2097. (page 20)

- [57] C. Chen, M.P. Deutscher, RNase R is a highly unstable protein regulated by growth phase and stress, *RNA* 16 (2010) 667–672. (page 20)
- [58] H. El-Samad, H. Kurata, J.C. Doyle, C.A. Gross, M. Khammash, Surviving heat shock: Control strategies for robustness and performance, *Proc. Natl. Acad. Sci. USA* 102 (2005) 2736–2741. (page 20)
- [59] J.L. Hargrove, Microcomputer-assisted kinetic modeling of mammalian gene expression, *FASEB J.* 7 (1993) 1163–1170. (page 20)
- [60] B. Alberts, A. Johnson, J. Lewis, M. Raff, K. Roberts, and P. Walter, *Molecular Biology of the Cell*, fourth ed., Garland Science, New York, 2002. (page 20)
- [61] J.A. Bernstein, A.B. Khodursky, P.-H. Lin, S. Lin-Chao, S.N. Cohen, Global analysis of mRNA decay and abundance in *Escherichia coli* at single-gene resolution using two-color fluorescent DNA microarrays, *Proc. Natl. Acad. Sci. USA*. 99 (2002) 9697–9702. (page 20)
- [62] I. Golding, J. Paulsson, S.M. Zawilski, E.C. Cox, Real-Time Kinetics of Gene Activity in Individual Bacteria, *Cell* 123 (2005) 1025–1036. (page 21)
- [63] D. Kennell, H. Riezman, Transcription and translation initiation frequencies of the *Escherichia coli* lac operon, *J. Mol. Biol.* 114 (1977) 1–21. (page 21)
- [64] F.C. Kafatos, The cocoonase zymogen cells of silk moths: a model of terminal cell differentiation for specific protein synthesis, *Curr. Topics Dev. Biol.* 7 (1972) 125–191. (page 21)
- [65] B.S. Laursen, H.P. Soerensen, K.K. Mortensen, H.U. Sperling-Petersen, Initiation of Protein Synthesis in Bacteria, *Microbiol. Mol. Biol. Rev.* 69 (2005) 101–123. (page 21)
- [66] L.L. Sampson, R.W. Hendrix, W.M. Huang, S.R. Casjens, Translation initiation controls the relative rates of expression of the bacteriophage λ late genes, *Proc. Natl. Acad. Sci. USA*. 85 (1988) 5439–5443. (page 21)
- [67] R. Young, H. Bremer, Polypeptide-chain-elongation rate in *Escherichia coli* B/r as a function of growth rate, *Biochem. J.* 160 (1976) 185–194. (page 21)
- [68] H. Bremer, J. Hymes, P.P. Dennis, Ribosomal RNA chain growth rate and RNA labelling patterns in *Escherichia Coli*, *J. Theor. Biol.* 45 (1974) 379–403. (page 21)
- [69] A.A. Cohen, T. Kalisky, A. Mayo, N. Geva-Zatorsky, T. Danon, I. Issaeva, R. B. Kopito, N. Perzov, R. Milo, A. Sigal, U. Alon, Protein Dynamics in Individual Human Cells: Experiment and Theory, *PLoS One* 4 (2009) e4901. (page 21)
- [70] A. Mortazavi, B.A. Williams, K. McCue, L. Schaeffer, B. Wold, Mapping and quantifying mammalian transcriptomes by RNA-Seq, *Nat. Meth.* 5 (2008) 621–628. (page 21)
- [71] G.A. Galau, W.H. Klein, R.J. Britten, E.H Davidson, Significance of rare mRNA sequences in liver, *Arch. Biochem. Biophys.* 179 (1977) 584–599. (page 21)
- [72] C.E. Sims, N.L. Allbritton, Analysis of single mammalian cells on-chip, *Lab Chip* 7 (2007) 423–440. (page 21)
- [73] S.P. Gygi, Y. Rochon, B.R. Franza, R. Aebersold, Correlation between protein and mRNA abundance in yeast, *Mol. Cell. Biol.* 19 (1999) 1720–30. (page 21)

Tables

Table 1. Model parameters

Name	Symbol	Non-dimensional value	Value for bacteria	Value for eukaryotes
transcriptional noise default value	ε_{01}	1/15		
translational noise default value	ε_{02}	1/75		
gene switching noise default value	σ_0	1/50		
transcriptional noise	ε_1		ε_{01}	$\varepsilon_{01}/5$
translational noise	ε_2		ε_{02}	$\varepsilon_{02}/25$
gene switching noise	σ		$\sigma_0/100$	σ_0
protein degradation	r_2	1	$10^{-4}/s$ ^(a)	$10^{-4}/s$ ^(b)
mRNA degradation	r_1	$10r_2$	$10^{-3}/s$ ^(c)	$10^{-3}/s$ ^(d)
inducible gene activation	c_2	$4.8r_2(\varepsilon_1\varepsilon_2)^2/\sigma$	$1.9 \times 10^{-6}/s$ ^(e)	$1.2 \times 10^{-12}/s$ ^(f)
basal gene activation	c_0	$0.027r_2/\sigma$	$0.0135/s$ ^(g)	$0.000135/s$ ^(g)
gene inactivation	b_0	r_2/σ	$0.5/s$ ^(g)	$0.005/s$ ^(g)
mRNA transcription	Q_1	r_1/ε_1	$0.015/s$ ^(h)	$0.075/s$ ⁽ⁱ⁾
protein translation	Q_2	r_2/ε_2	$0.0075/s$ ^(j)	$0.1875/s$ ^(k)
mRNA number in inactive (active) state		$0.03/\varepsilon_1$ $(0.64/\varepsilon_1)$	0.5 (10.6) ^(l)	2.28 (53.2) ^(m)
protein number in inactive (active) state		$0.03/\varepsilon_1\varepsilon_2$ $(0.64/\varepsilon_1\varepsilon_2)$	34.3 (798.4) ⁽ⁿ⁾	4290.1 (99799.4) ^(o)

^(a)Most of bacterial proteins are very stable, with degradation rate constants: $1.4 \times 10^{-5}/s \div 5.6 \times 10^{-5}/s$ [56]. Some proteins have much higher degradation rates. E. coli RNase R has degradation rate constant of $10^{-3}/s$ (in exponential phase) [57], factor σ^{32} has degradation rate constant of $10^{-2}/s$ (in steady-state growth phase) [58].

^(b)Mammals: protein degradation rate constants: $1.7 \times 10^{-6}/s \div 1.7 \times 10^{-3}/s$ [59].

^(c)The vast majority of mRNAs in a bacterial cell are very unstable, having a half-life of about 3 minutes (decay rate constant $3 \times 10^{-3}/s$) [60]. E. coli: mRNA half-lives span between 1 and 18 minutes (decay rate constants $10^{-2}/s \div 6 \times 10^{-4}/s$) [61].

^(d)The eukaryotic mRNAs are more stable than prokaryotic with half-lives exceeding 10 hours (decay rate constant $2 \times 10^{-5}/s$). However many have half-lives are of order of 30 minutes (decay rate constant $3 \times 10^{-4}/s$) or less [60]. Mammalian mRNA degradation rate constants: $1.7 \times 10^{-5}/s \div 1.7 \times 10^{-3}/s$ [59].

- (*e*) For $1 \mu\text{m}^3$ cell volume (bacterial cell) $c_2 = 6.9/(\mu\text{M}^2 \times \text{s})$.
- (*f*) For $2 \times 10^3 \mu\text{m}^3$ cell volume (mammalian cell) $c_2 = 1.7/(\mu\text{M}^2 \times \text{s})$.
- (*e*),(*f*),(*g*) For prokaryotes gene switching is faster than for eukaryotes [2]. Slow gene switching in eukaryotes is causing large mRNA bursts [5]. However, the transcriptional bursting was also observed at E. coli promoter [62].
- (*h*) For E. coli the maximal transcription rate constant: $0.84/\text{s}$ [63].
- (*i*) For eukaryotes the maximal transcription rate constant: $0.84/\text{s}$ [64].
- (*j*) Translation initiation intervals are specific for each mRNA [65]. E. coli: translation initiation rate constant may vary at least 1000-fold [66]; examples of translation initiation frequencies; β -galactosidase: $0.31/\text{s}$ (spacing between ribosomes: 110 nucleotides), galactoside acetyltransferase: $0.06/\text{s}$ (spacing between ribosomes: 580 nucleotides) [63]; maximal peptide chain elongation rate: $20\text{aa}/\text{s}$ [67, 68]; average peptide chain elongation rate: $12\text{aa}/\text{s}$ [63].
- (*k*) Translation rate constant for eukaryotes: $0.018/\text{s} \div 1.8/\text{s}$ [69].
- (*l*) E. coli: average mRNA copy number: $10^{-4} \div 5$ molecules/cell [13].
- (*m*) Mammals (mice): average mRNA copy number observed in natural transcriptomes: $0.5 \div 5 \times 10^4$ molecules/cell [70], [71].
- (*n*) E. coli: average protein copy number: $10^{-1} \div 10^4$ molecules/cell [13].
- (*o*) Mammals: the maximal protein copy number: 10^8 molecules/cell [72]. Most of yeast genes: $10^3 - 5 \times 10^4$ molecules/cell [73].

Figures

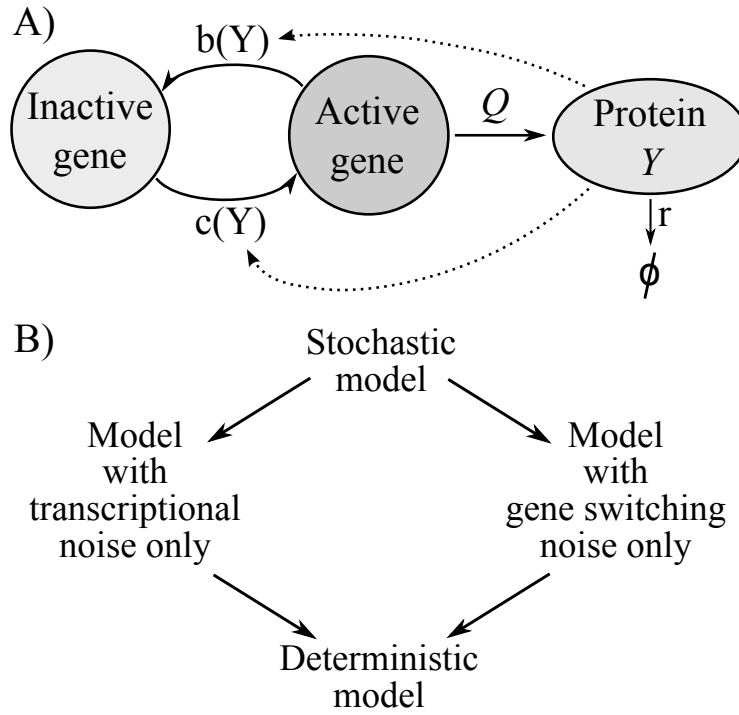


Figure 1. Two-stage gene expression model. (A) Schematic of the model (B) Stochastic model and its three approximations.

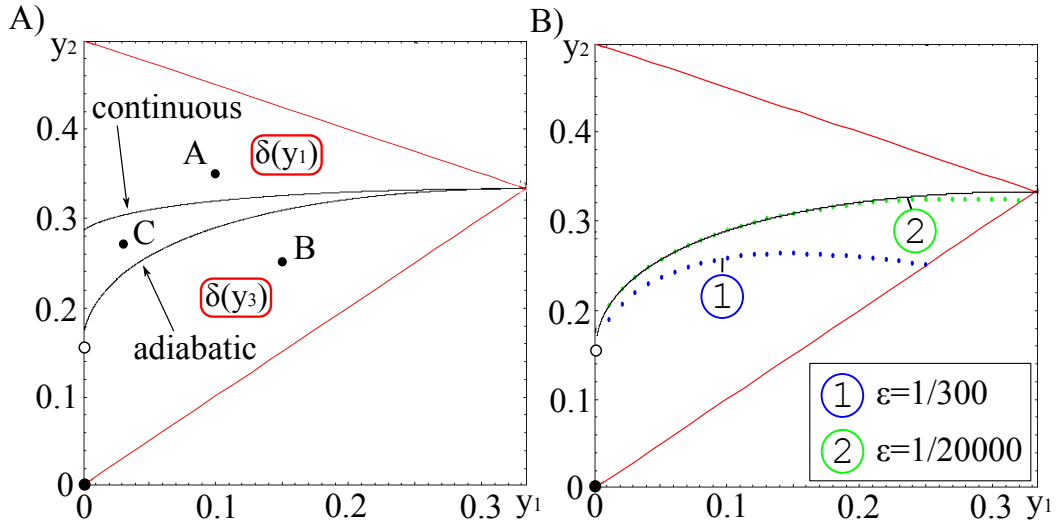


Figure 2. Bistability domain in $\{y_1, y_2\}$ space. Panel (A): the two black curves divide the domain into three subdomains: in the subdomain \mathcal{A} (containing point A), the SPDs of adiabatic and continuous approximations concentrate in y_1 ; in the subdomain \mathcal{B} (containing point B), the SPDs of the two approximations concentrate in y_3 . In the subdomain \mathcal{C} (bounded by separatrices $S_{\text{adiabatic}}$ and $S_{\text{continuous}}$), the SPD for the continuous approximation ($\varepsilon = 0$) is concentrated in y_3 while the SPD for the adiabatic approximation ($\sigma = 0$) is concentrated in y_1 . Panel (B): continuous line – analytically calculated division curve $y_2(y_1)$ for the adiabatic approximation ($\sigma = 0$) in the $\varepsilon \rightarrow 0$ limit; dotted lines are the separation lines for a finite noise parameter $\varepsilon = 1/300$ and $\varepsilon = 1/20000$.

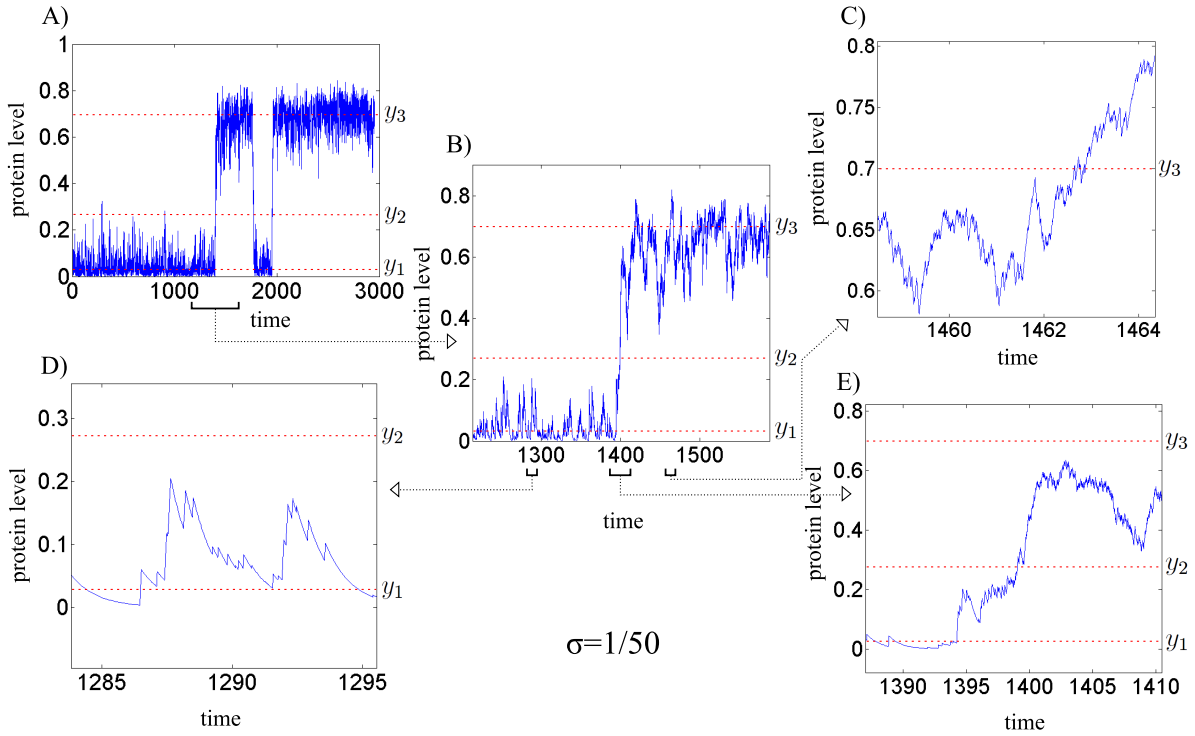


Figure 3. Two-stage model: Stochastic simulation trajectory for continuous approximation, $\varepsilon = 0$. Protein level obtained in the numerical simulation for $\sigma = 1/50$. The three steady states $y_1 = 0.03$ (stable), $y_2 = 0.27$ (unstable) and $y_3 = 0.7$ (stable) of the deterministic approximation are shown by the dashed lines. For such y_1, y_2, y_3 (corresponding to point C in Fig. 2A) the SPD of the continuous approximation converges to $\delta(y_3)$ as $\sigma \rightarrow 0$, see Fig. 5C. Time is given in units in which the protein degradation rate constant is equal to 1. Panel (B) shows the zoomed region from Panel (A) around transition from the low to the high protein level, the further detail of this transition is shown in Panel (E); Panel (D) shows the trajectory in the vicinity of the steady state y_1 ; Panel (C) shows the trajectory in the vicinity of steady state y_3 .

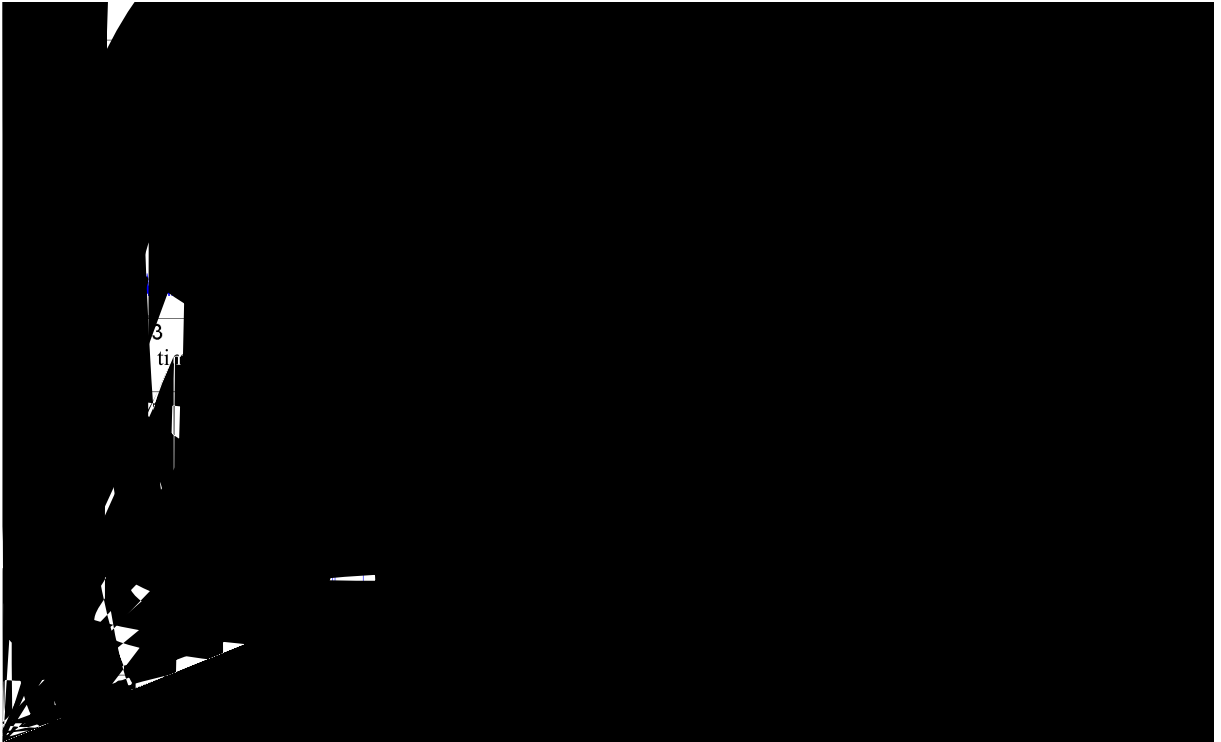


Figure 4. Two-stage model: Stochastic simulation trajectory for adiabatic approximation, $\sigma = 0$. Protein level obtained in the numerical simulation for $\varepsilon = 1/100$. The three steady states $y_1 = 0.03$ (stable), $y_2 = 0.27$ (unstable) and $y_3 = 0.7$ (stable) of the deterministic approximation are shown by the dashed lines. For such y_1, y_2, y_3 (corresponding to point C in Fig. 2A) the SPD of the adiabatic approximation converges to $\delta(y_1)$ as $\varepsilon \rightarrow 0$, see Fig. 5C. Panel (B) shows the zoomed region from Panel (A) around transition from the low to high protein level, the detail of this transition is shown in Panel (E); Panel (D) shows the trajectory in the vicinity of the steady state y_1 ; Panel (C) shows the trajectory in the vicinity of the steady state y_3 .

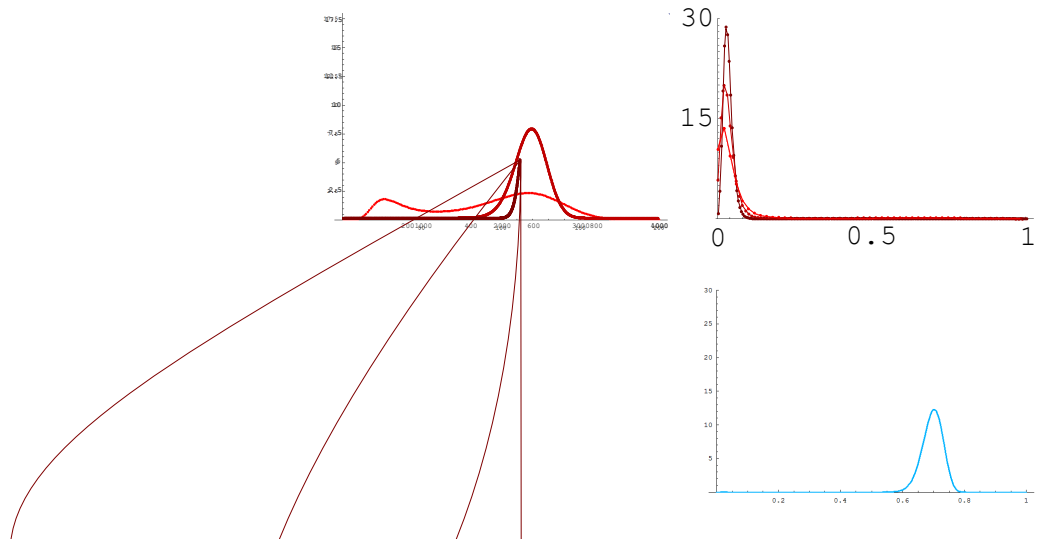


Figure 5. The SPDs for the adiabatic and continuous approximations. Columns A, B and C correspond to points A , B and C in Fig. 2A. Upper row panels – the adiabatic approximation, lower row panels – the continuous approximation. For $y_1 = 0.03$, $y_2 = 0.27$, in the zero noise limit (column C), the SPDs of the adiabatic and the continuous approximations converge, respectively to $\delta(y_1)$, and $\delta(y_3)$.

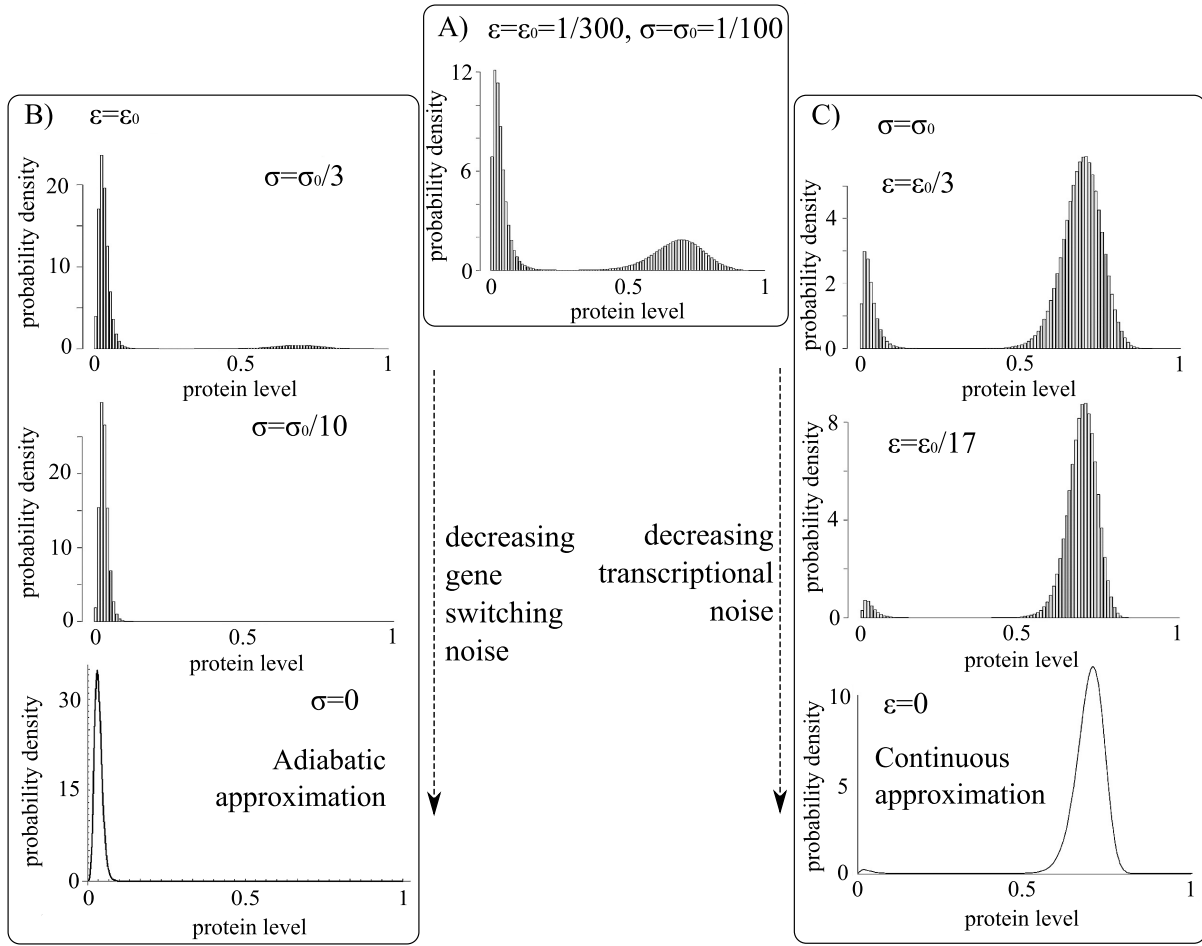


Figure 6. The SPD of the two-stage model obtained in Monte Carlo simulations for $y_1 = 0.03$, $y_2 = 0.27$ (point *C* in Fig. 2A). Panel (A) shows bimodal SPD in the case when the magnitudes of two types of noise are comparable: $\varepsilon_0 = 1/300$, $\sigma_0 = 1/100$. Panel (B) consisting of three subpanels shows the SPD for the constant transcriptional noise ε_0 and decreasing gene switching noise σ . Panel (C) also consisting of three subpanels, shows the SPD for the constant gene switching noise σ_0 and decreasing transcriptional noise ε . The lowest subpanels show the analytically calculated SPDs for the adiabatic and continuous approximations.

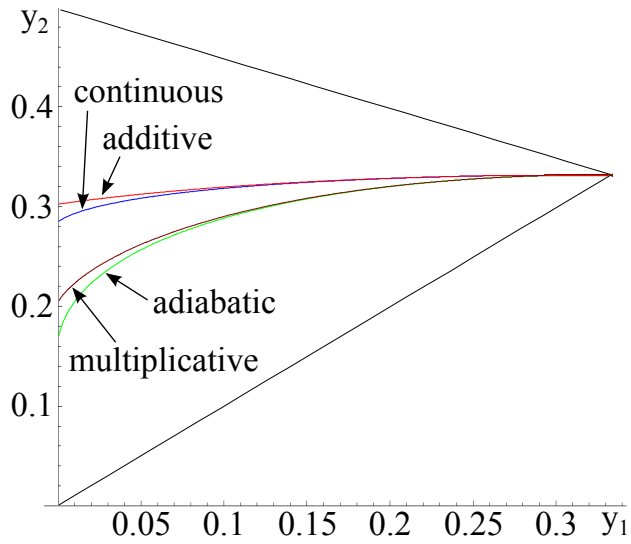


Figure 7. Separatrices calculated for continuous and adiabatic approximations (as in Fig. 2A) compared with those resulting from Fokker-Plank equation with assumed either additive or multiplicative noise. For each of approximations for y_1, y_2 above the separatrix, the global attractor is in y_1 , while for y_1, y_2 below the separatrix the global attractor is in y_3 .

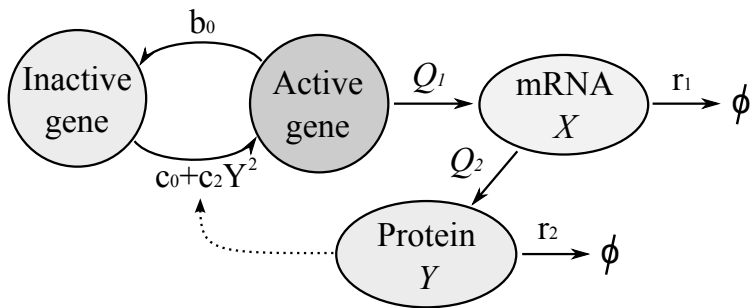


Figure 8. Schematic of the three-stage model.

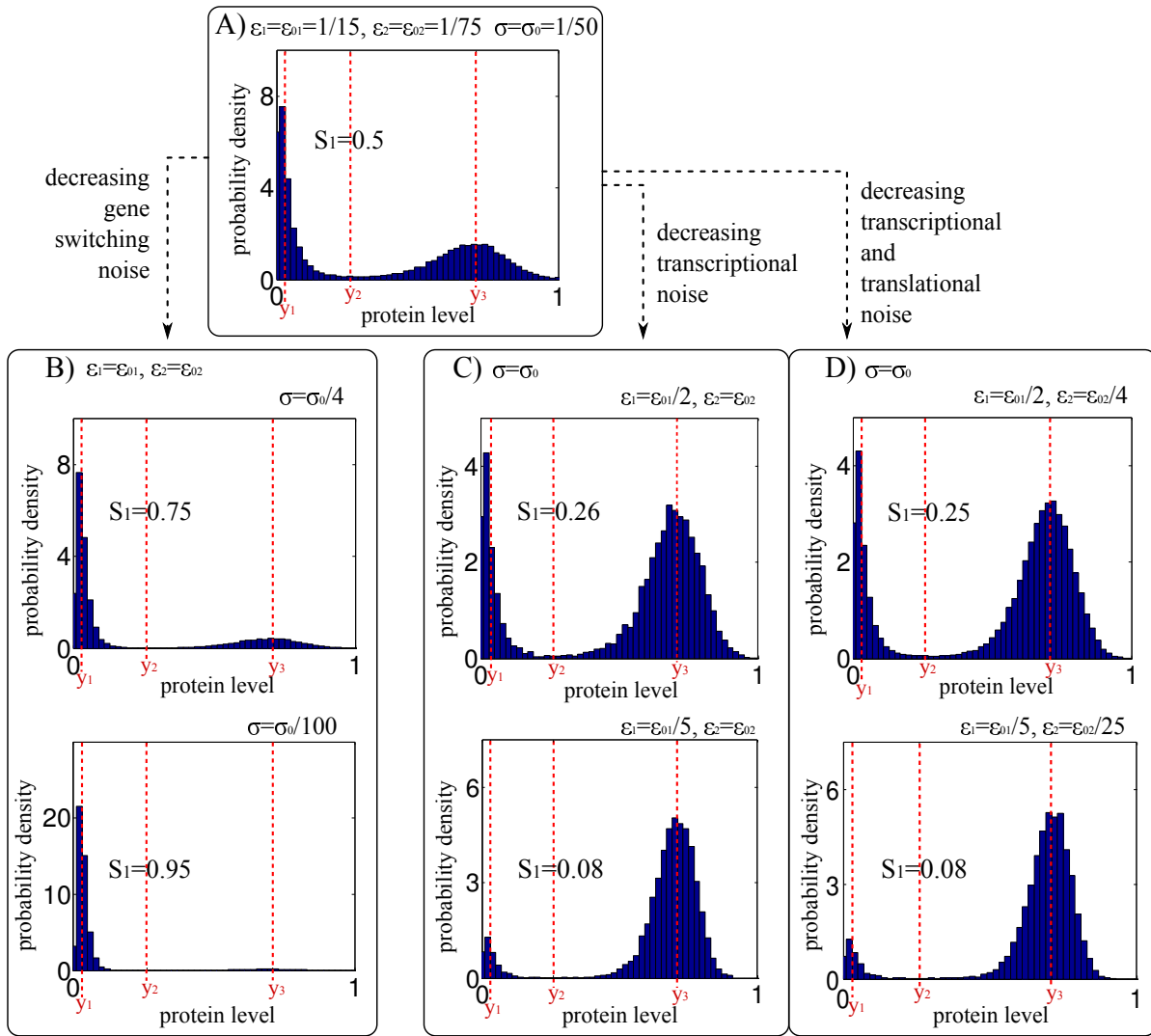


Figure 9. The marginal SPD of the three-stage model for parameters from Table 1. S_1 – mass fraction in the inactive state basin of attraction. Panel (A) shows almost “equimodal” SPD obtained for in the case when $\epsilon_{01} = 1/150$, $\epsilon_{02} = 1/75$ and $\sigma_0 = 1/50$. Panel (B) shows the SPD of the constant transcriptional and translational noise $\epsilon_1 = \epsilon_{01}$, and $\epsilon_2 = \epsilon_{02}$ and decreasing gene switching noise σ . Panel (C) shows the SPD for the constant gene switching noise $\sigma = \sigma_0$, constant translational noise $\epsilon_2 = \epsilon_{02}$ and decreasing transcriptional noise ϵ_1 . Panel (D) shows the SPD for the constant gene switching noise $\sigma = \sigma_0$ and decreasing transcriptional and translational noise parameters ϵ_1 and ϵ_2 .

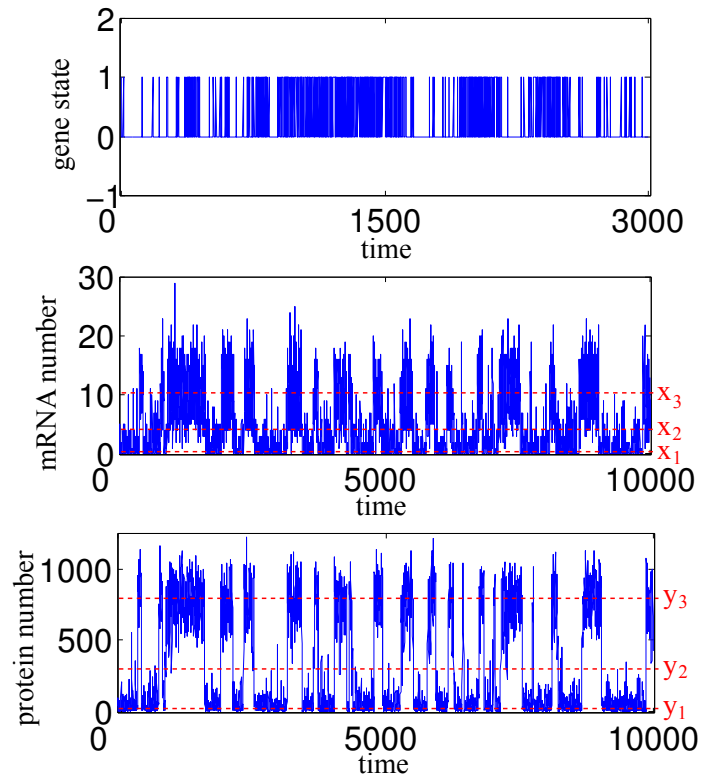


Figure 10. Three-stage model: Stochastic simulation trajectory for default noise parameters $\varepsilon_1 = \varepsilon_{01} = 1/150$, $\varepsilon_2 = \varepsilon_{02} = 1/75$ and $\sigma = \sigma_0 = 1/50$. The corresponding SPD is shown in Fig. 9A. Time is given in units equal to the mean protein lifetime.

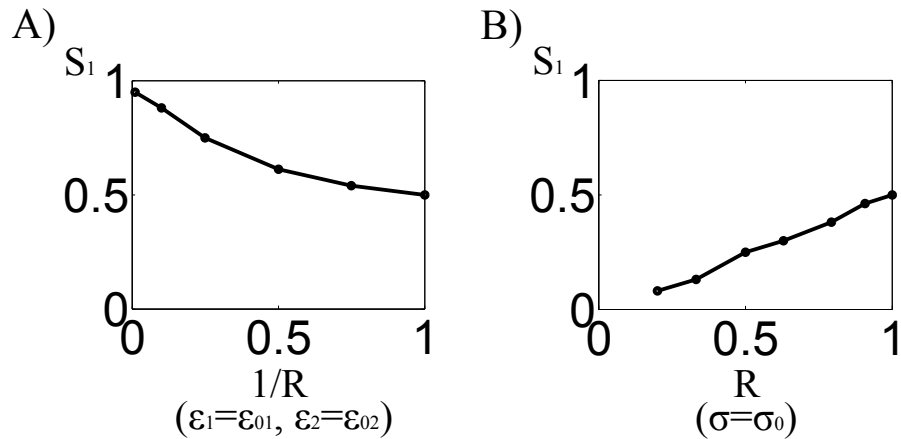


Figure 11. Mass fraction in the vicinity of the inactive state, S_1 , as a function of noise parameters ratio $R = \frac{\varepsilon_1/\varepsilon_{01}}{\sigma/\sigma_0}$. Panel (A) S_1 plotted as a function of R^{-1} for constant $\varepsilon_1 = \varepsilon_{01}$ (and $\varepsilon_2 = \varepsilon_{02}$). Panel (B) S_1 as a function of R for constant $\sigma = \sigma_0$.